Apical Spectrin Is Essential for Epithelial Morphogenesis but Not Apicobasal Polarity in *Drosophila*

Daniela C. Zarnescu*‡ and Graham H. Thomas*‡

*Department of Biology and ‡Department of Biochemistry and Molecular Biology, The Pennsylvania State University, University Park, Pennsylvania 16802

Abstract. Changes in cell shape and position drive morphogenesis in epithelia and depend on the polarized nature of its constituent cells. The spectrin-based membrane skeleton is thought to be a key player in the establishment and/or maintenance of cell shape and polarity. We report that apical β_{Heavy}-spectrin (β_H), a terminal web protein that is also associated with the *zonula adherens*, is essential for normal epithelial morphogenesis of the *Drosophila* follicle cell epithelium during oogenesis. Elimination of β_H by the *karst* mutation prevents apical constriction of the follicle cells during mid-oogenesis, and is accompanied by a gross breakup of the *zonula adherens*. We also report that the integrity of the migratory border cell cluster, a group of anterior follicle cells that delaminates from the follicle epithelium, is disrupted.

Elimination of β_H prevents the stable recruitment of α-spectrin to the apical domain, but does not result in a loss of apicobasal polarity, as would be predicted from current models describing the role of spectrin in the establishment of cell polarity. These results demonstrate a direct role for apical $(\alpha\beta_H)_2$-spectrin in epithelial morphogenesis driven by apical contraction, and suggest that apical and basolateral spectrin do not play identical roles in the generation of apicobasal polarity.

Key words: spectrin • oogenesis • cell polarity • zonula adherens • morphogenesis

EPITHELIAL cell sheets perform a number of coordinated morphogenetic movements in response to a variety of signals during the development of multicellular organisms. These include infoldings generated by localized apical constriction and concerted migrations driven either by convergent extension or radial intercalation (Gumbiner, 1992). Apicobasal membrane polarity, a hallmark of epithelial cells, is essential for generating such movements as well as for the interaction of the cell sheet with surrounding tissues. The cadherin-based junctional complex, the *zonula adherens* (ZA),[1] which lies at the boundary separating the apical and basolateral membrane domains, functions to link polarity and morphogenesis. The ZA plays at least three distinct structural roles in an epithelium. First, it is a major source of cell–cell adhesion, and is thus important for the integrity of the epithelium; second, the contraction and remodeling of the ZA is an essential step in cell sheet morphogenesis; and third, by preventing the passive diffusion of integral membrane proteins between the apical and basolateral domains, the ZA is also a major contributor to cell polarity (Gumbiner, 1996; Knust and Leptin, 1996).

The spectrin-based membrane skeleton (SBMS) is a ubiquitous cytoskeletal structure that has been postulated to play a role in the establishment and/or maintenance of apicobasal polarity and has a close relationship with cadherin-based adhesive complexes (McNeill et al., 1990; Nelson et al., 1990; Lombardo et al., 1994; Thomas et al., 1998; Yeaman et al., 1999). The SBMS was first identified as a dense meshwork of proteins that confers the biconcave shape on erythrocytes (reviewed in Bennett and Gilligan, 1993). In electron micrographs, the erythrocyte membrane skeleton has a lattice-like organization of five- and six-sided polygons comprised of flexible 200-nm spectrin molecules, with short actin filaments at the vertices. This network is linked to integral membrane proteins via spectrin-binding proteins such as ankyrin and protein 4.1 (Bennett and Gilligan, 1993). Other proteins such as adducin regulate the stability of the SBMS by modulating the spectrin–actin interaction (Matsuoka et al., 1996). This structure is also subject to regulation by phosphorylation and proteolysis (Cohen and Gascard, 1992) and exhibits changes in subcellular localization consistent with a role in the modulation of cell shape during epithelial morphogenesis

Address correspondence to Graham H. Thomas, Departments of Biology and of Biochemistry and Molecular Biology, The Pennsylvania State University, 208 Erwin W. Mueller Laboratory, University Park, PA 16802. Tel.: (814) 863-0716. Fax: (814) 865-9131. E-mail: gxt5@psu.edu

1. *Abbreviations used in this paper:* β_H, β_{Heavy}-spectrin; SBMS, spectrin-based membrane skeleton; ZA, *zonula adherens*.

(Sadler et al., 1986; Thomas and Kiehart, 1994; Wessel and Chen, 1993). Most of the key components of the erythrocyte SBMS have isoforms or counterparts in nonerythroid tissues, including epithelia.

Several properties of the SBMS have led to the proposal that it plays a key role in the generation and/or maintenance of apicobasal cell polarity in epithelia (Yeaman et al., 1999). First, the SBMS has the ability to bind to and retain specific proteins in specific membrane domains (Hammerton et al., 1991) providing a mechanism for the generation and/or maintenance of asymmetric protein distributions. Second, different spectrin isoforms define different membrane domains (Glenney and Glenney, 1983; Lazarides et al., 1984; Dubreuil et al., 1997; Lee et al., 1997; Thomas et al., 1998), consistent with their proposed role in establishing such asymmetry. Third, the SBMS is an early recruit to sites of cadherin-based cell adhesion complexes that form as the initial step in the regulatory cascade that generates apicobasal polarity (Yeaman et al., 1999). Finally, spectrin and novel spectrin-like proteins may participate directly in protein sorting via direct association with the secretory apparatus at the Golgi, on vesicles, or at the plasma membrane (Holleran et al., 1996; Sikorski et al., 1991; Beck et al., 1994; DeMatteis and Morrow, 1998).

Each spectrin molecule is comprised of two α and two β chains that are largely made up of spectrin repeats that give the molecules their extended rope-like morphology (Speicher and Marchesi, 1984; Yan et al., 1993), while an actin binding domain at the NH_2 terminus of the β-chain permits $(\alpha\beta)_2$ tetramers to cross-link F-actin. The presence of specialized spectrin repeats and of various nonrepetitive domains that provide binding sites for other proteins suggests that these molecules act as molecular scaffolds capable of nucleating specific complexes of proteins at the membrane (Bennett and Gilligan, 1993; Viel and Branton, 1996; DeMatteis and Morrow, 1998).

In *Drosophila melanogaster*, the SBMS is built around two distinct spectrin isoforms; a single α-spectrin chain assembles with one of two β-spectrin chains, β- or β_{Heavy}-spectrin (β_H), to form $(\alpha\beta)_2$ and $(\alpha\beta_H)_2$ tetramers, respectively. Fly β-spectrin has a typical β-spectrin–like organization with an NH_2-terminal actin binding domain followed by 17 spectrin repeats and a nonrepetitive COOH-terminal region containing a pleckstrin homology (PH) domain (Byers et al., 1992). In contrast, β_H contains 30 spectrin repeats, an Src homology 3 (SH3) domain, and unique sequences surrounding the PH domain in the COOH terminus (Dubreuil et al., 1990; Thomas et al., 1997). $(\alpha\beta)_2$ and $(\alpha\beta_H)_2$ tetramers form actin cross-linking units of 180 and 250 nm, respectively, reflecting the difference in the number of spectrin repeats within each β chain (Dubreuil et al., 1990). In keeping with the proposed role of the SBMS in cell polarity, *Drosophila* spectrins are polarized in epithelia, such that $(\alpha\beta)_2$ is always basolateral while $(\alpha\beta_H)_2$ is always apical (Dubreuil et al., 1997, 1998; Lee et al., 1997; Thomas et al., 1998). $(\alpha\beta_H)_2$ is associated with the ZA where its abundance closely follows that of *D*E-cadherin (Thomas et al., 1998; Thomas and Williams, 1999), but is also found across the whole apical domain in regions of apical constriction (Thomas and Kiehart, 1994), and in the terminal web subtending apical microvillar brush borders (Dubreuil et al., 1998; Thomas et al., 1998).

The SBMS is essential for *Drosophila* development. Mutations have been recovered in all three spectrin genes and all result in extensive or complete lethality. Mutations affecting α-spectrin are first instar larval lethals that disrupt both the apical and basolateral SBMS, resulting in the disruption of cell–cell contact (Lee et al., 1993), aberrant acidification of the gut lumen (Dubreuil et al., 1998), and defects in both somatic and germline cells during oogenesis (Deng et al., 1995; de Cuevas et al., 1996; Lee et al., 1997). Mutations affecting the conventional β-spectrin isoform are late embryonic lethals (Goldstein, L.S.B., and R.R. Dubreuil, personal communication) while mutations in *karst*, the locus that encodes β_H, result in widespread larval lethality and defects in tissues of epithelial origin (Thomas et al., 1998). The *karst* phenotype exhibits conspicuous variable expressivity even in null alleles, and mutations in the homologous gene in *Caenorhabditis elegans* are viable (McKeown et al., 1998).

Here, we examine the specific contribution of the apical SBMS to epithelial cell polarity, adhesion, and morphogenesis by analyzing the effects of the *karst* mutation on follicle cell morphogenesis in *Drosophila* oogenesis. During mid-oogenesis, the follicle cell epithelium undergoes a well-defined migration to envelop the oocyte. This involves apical constriction and results in a change in cell shape from cuboidal to columnar. We show that the *karst* mutation completely eliminates the apical spectrin membrane skeleton and prevents normal apical contraction of the follicle cells. However, lack of apical spectrin does not eliminate the ability of these cells to establish and maintain apicobasal polarity. Furthermore, we observe gross disruptions of the ZA in *karst* mutants. These results are consistent with the hypothesis that a primary role of the apical SBMS lies in facilitating changes in cell shape, perhaps by contributing to the integrity of the ZA. Our results also imply that it is the disruption of the basolateral SBMS specifically, or the basolateral plus the apical SBMS, that results in the loss of apicobasal polarity seen in α-spectrin mutants (Lee et al., 1997). Surprisingly, we also observe a disruption of the migratory border cell cluster in *karst* mutants that suggests a role for β_H in their delamination from the follicular epithelium.

Materials and Methods

Fly Stocks

The *karst* stocks *mwh ve* kst^1 *e/TM6B*, *mwh ve* kst^2 *e/TM6B*, *mwh* $kst^{14.1}$ *red e/TM6B*, *mwh Df(3L)1226 red e/TM6B*, and kst^{01318}*/TM6B* have been previously described (Thomas et al., 1998). The recombinant stocks *mwh* $kst^{1\text{-}1151}$ *FRT80B/TM6B* and *mwh* $kst^{2\text{-}2119}$ *FRT80B red/TM6B* were derived from the above stocks by recombination with the *rucuca* chromosome (Lindsley and Zimm, 1992) to remove ancillary lethals and to *w*; *FRT80B* (Xu and Rubin, 1993) for other purposes. The $slbo^1$*/CyO* stock was a gift from Dr. D. Montell (Johns Hopkins University) and was introduced into the *karst* mutant background by standard genetic methods.

Antibodies

To detect β_H, we used serum #243 (Thomas and Kiehart, 1994) at 1/200. To detect α-spectrin, we used ascites fluid #N3 at a dilution of 1/5,000 (Byers et al., 1987). To detect β-spectrin, we used rabbit serum #89 (Byers et al., 1989) at a dilution of 1/200. To detect *D*E-cadherin, we used the mono-

clonal antibody #DCAD2 (Uemura et al., 1996) at a dilution of 1/20. To detect myosin IB, we used affinity-purified rabbit antibodies (Morgan et al., 1995) at a dilution of 1/200. To detect Notch, we used the monoclonal antibody 9C6 (Wharton et al., 1985) at 1/200. To detect cytoplasmic myosin II, we used the rabbit serum #656 (Kiehart and Feghali, 1986) at 1/200. To detect Fasciclin III, we used the monoclonal antibody 7G10 (Patel et al., 1987; obtained from the Developmental Studied Hybridoma Center) at 1/10.

FITC, Cy3 or Cy5 conjugated, and affinity-purified secondary antibodies used were all made in goat and were obtained from Jackson ImmunoResearch Laboratories, Inc. These antibodies were rehydrated according to the manufacturer's instructions and used at dilutions of 1/100. Alexa 488 conjugated secondary antibody was obtained from Molecular Probes and used at a dilution of 1/200.

Immunofluorescent Staining of Ovaries

2–4-d old females fed with yeast paste at 25°C were dissected and their ovaries were teased apart into individual ovarioles in PBS (130 mM NaCl, 7 mM Na_2HPO_4, 3 mM NaH_2PO_4, pH 7) using a tungsten needle. The tissue was fixed in buffer B (16.7 mM KH_2PO_4/K_2HPO_4, pH 6.8, 75 mM KCl, 25 mM NaCl, 3.3 mM $MgCl_2$, 5% paraformaldehyde; Freeman et al., 1986) for 15–20 min at room temperature. After a 30-min wash in PBT (10 mM Na_2HPO_4/NaH_2PO_4, pH7.4, 175 mM NaCl, 0.1% Triton X-100), samples were blocked in PBT-NGS (PBT, 5% normal goat serum). The samples were then incubated in PBT-NGS containing the primary antibody for 4–5 h at room temperature or overnight at 4°C. After one wash in PBT and one wash in PBT-NGS for 30 min each, the samples were incubated in PBT-NGS with the appropriate secondary antibody for 2–3 h at room temperature or overnight at 4°C. After two washes in PBS, the stained ovaries were equilibrated and mounted in mounting medium (100 mM Tris-Cl, pH 8.5, 80% glycerol, 2% *n*-propyl gallate). To costain for F-actin, samples were further incubated for 30 min at room temperature in 165 nM FITC- or TRITC-phalloidin (Molecular Probes) in the first wash after secondary antibody incubation. Nuclei were visualized by staining with 5 μg/ml propidium iodide in PBT for 20 min at room temperature (de Cuevas et al., 1996).

Activity Staining for β-Galactosidase

Ovaries were dissected in PBS and fixed in 1% glutaraldehyde in PBS for 20 min at room temperature. After three to four washes in PBS, the tissue was incubated in prewarmed reaction solution (10 mM sodium phosphate, pH 7.2, 150 mM NaCl, 1 mM $MgCl_2$, 3 mM $K_3Fe(CN)_6$, 3 mM $K_4Fe(CN)_6$, 0.1% X-Gal) for at least 30 min at 37°C. The samples were extensively washed in PBS and mounted in mounting medium.

Sample Imaging

Imaging of immunofluorescently stained ovaries was done using an MRC1024 confocal microscope (Bio-Rad Laboratories). Imaging of ovaries stained for β-galactosidase activity was done on a BX50 microscope (Olympus Corp.) equipped with a Dage/MTI CCD72T camera and DSP2000 signal processor, and were imported directly into a Power Macintosh 8100/80AV (Apple Computer) using a DT2255 frame grabber (Data Translations) controlled by the public domain program NIH Image (v1.61 available on the internet at http://rsb.info.nih.gov/nih-image). Images were contrast stretched as appropriate using Adobe Photoshop v4.0 (Adobe Systems, Inc.) and the figures assembled and annotated in Adobe Illustrator v6.0.

Morphometric Analysis

Images of sagittal optical sections of 81 wild-type and 318 *karst* mutant egg chambers at stage 9 or 10A (a comprehensive combination of kst^1, kst^2, $kst^{14.1}$, and kst^{01318} alleles over one another and over *Df(3L)1226*), that had been stained for α-spectrin, *D*E-cadherin, actin, or Notch, were acquired. The distances described in text and Fig. 2 were then measured and analyzed using Excel 98 (Microsoft Corp.) and/or Deltagraph (DeltaPoint, Inc.).

Measurement of Apical Surface Areas of Follicle Cells

To measure the follicle cell apical surfaces, we stained wild-type and kst^{01318} egg chambers for *D*E-cadherin to outline the apical contours. To ensure that only cells being viewed en face were measured, the following procedure was used. The z-axis motor on the confocal was stepped gradually out from the sagittal plane of the oocyte towards the apical domain of the upper follicle cell monolayer until the oocyte had just disappeared. Measurement of the apical surface areas was done using NIH Image software. Specifically, we used the Threshold option to isolate the cell outlines, after which the Measure option was used to quantify the number of pixels per apical surface per cell. Any breaks in the *D*E-cadherin staining, particularly in *karst* mutant egg chambers, were manually closed with straight, one pixel-wide lines before area measurement. The position of the center of each cell measured relative to the nurse cell/oocyte boundary was also recorded for each cell.

Results

The Distribution of β_H during Drosophila Oogenesis

Oogenesis in flies takes place in ovaries formed of 12–16 ovarioles, each of which consists of an anterior structure called the germarium and several egg chambers sequentially ordered with regard to their developmental stage (for review, see Spradling, 1993; see Fig. 1 A for example). The germarium is comprised of three zones (Fig. 1 B). In zone 1, two germline stem cells divide asymmetrically to give rise to a cystoblast and a stem cell. The cystoblast then divides synchronously four times to produce 16 cell cysts interconnected by ring canals as a result of incomplete cytokinetic events. In zone 2, 16 cell cysts become surrounded by a pool of follicle cells produced by asymmetric division of two to three somatic stem cells. By this stage, 1 of the 16 germ cells has adopted an oocyte fate and becomes located at the posterior of the cyst. The remaining 15 nurse cells undergo polytenization. In zone 3, fully formed stage 1 egg chambers begin to emerge from the germarium, bounded by a well polarized follicular epithelium (Fig. 1 A). Egg chambers will continue to grow and increase in size up to stage 9, while the follicle cell monolayer accommodates this growth by a series of cell divisions.

At the onset of stage 9, after all divisions have ceased, the majority of the follicle cell monolayer undergoes a concerted migration towards the posterior of the egg chamber onto the oocyte membrane. Those follicle cells that are left behind become squamous and continue to reside on the nurse cells. During this morphogenetic event, the migratory follicle cells undergo a change in cell shape from cuboidal to columnar, a process that is instrumental in accommodating them on the growing oocyte membrane. Concomitantly, a group of 6–10 anterior follicle cells called border cells round up (Fig. 1 A, * in stage 9) and plunge in between the nurse cells to reach the anterior of the oocyte (Fig. 1 A; * in stage 10). After the follicle cell monolayer and the border cells have reached the anterior of the oocyte, a specialized subset of follicle cells called centripetal cells migrate along the nurse cell–oocyte interface such that the follicle cells now completely surround the oocyte. Communication between nurse cells and the oocyte is maintained via ring canals that remain open until the nurse cells dump their cytoplasmic contents into the oocyte at stage 11.

Although two partial descriptions of the distribution of β_H during oogenesis have been published by other groups (de Cuevas et al., 1996; Lee et al., 1997), no complete description exists. We therefore began by fully characterizing the distribution of β_H in developing wild-type ovarioles

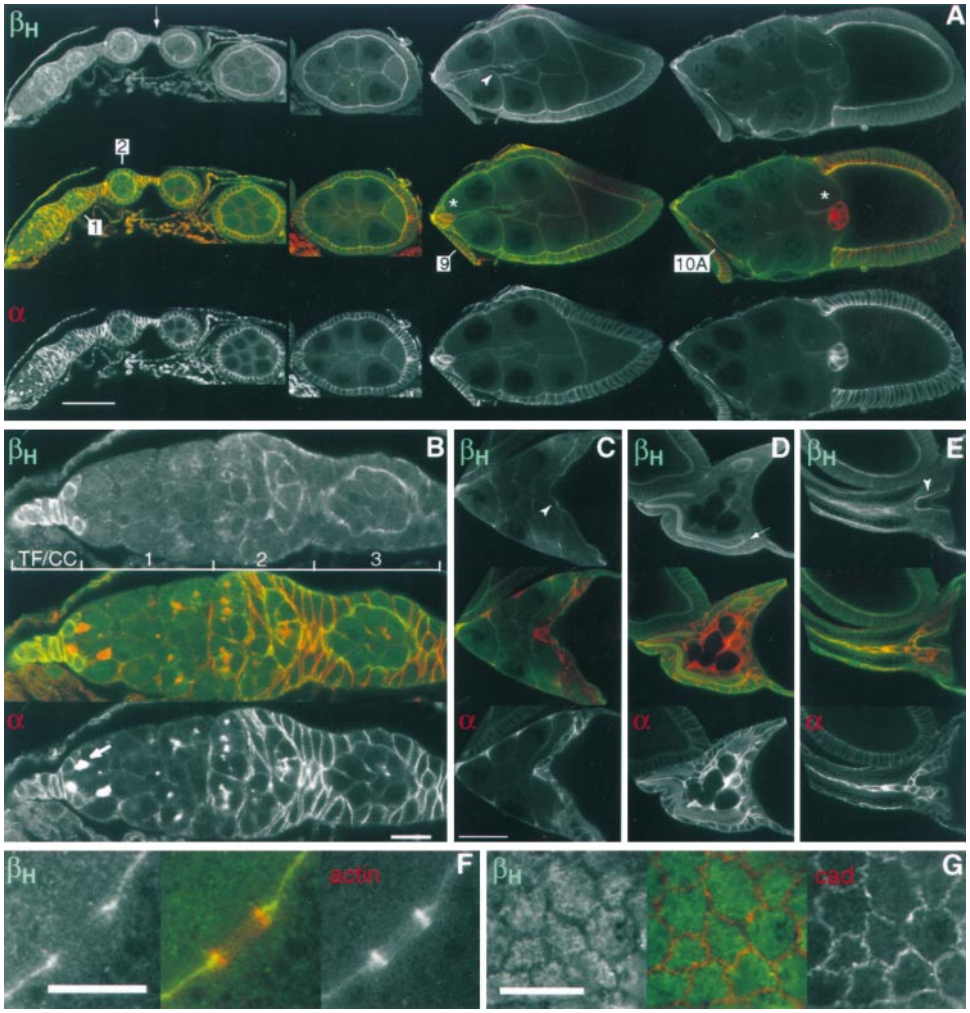

Figure 1. β_H distribution during oogenesis. (A–E) Wild-type ovariole costained for β_H (top) and α-spectrin (bottom). The middle panels are merged false color images with β_H in green and α-spectrin in red. Representative chambers for stages 1–10 are shown. Specific stages are indicated by the boxed numbers. (A) β_H is uniformly distributed along the germ cell membranes and is apically polarized in the follicle cell monolayer. β_H is also strongly expressed in stalks (arrow) and exhibits a patchy distribution on the border cell track during stage 9 (arrowhead). Scale bar, 50 μm. (B) High magnification view of a wild-type germarium indicating the location of zones 1–3. β_H is strongly expressed in the terminal filament and cap cells (TF/CC) but is absent from fusomes marked by α-spectrin (arrow). Scale bar, 10 μm. (C) Nurse cell cluster of a stage 11 egg chamber. β_H is seen faintly in filamentous structures within the dumping nurse cells. β_H reappears at the apical domain of the border cells (arrowhead; see also E). Scale bar, 50 μm in C–E. (D and E) Anterior ends of stages 12, 13, and 14 egg chambers, respectively. β_H is strongly expressed at the apical surface of follicle cells that are actively secreting chorion (arrow in D indicates the cells forming the dorsal appendages; arrowheads in C and E point to the border cells that secrete the micropyle). The nurse cells between the emerging dorsal appendages in D are undergoing programmed cell death. (F) High magnification view of a ring canal showing a slight enrichment of β_H (left) on the outer rim of this actin rich structure (right). (G) *En face* high magnification view of the apical domain of follicle cells showing β_H at the terminal web (left) and *D*E-cadherin (right) at the ZA. The central panels in F and G are merged false color images with the left and right panels of each in green and red, respectively. Bars: (F and G) 10 μm.

(Fig. 1). β_H expression in the germline is low to undetectable in the most anterior region of the germarium, and first appears in zone 2 (Fig. 1 B). In zone 3, fully formed stage 1 egg chambers emerge, β_H is found uniformly along the nurse cell and oocyte membranes (Fig. 1 B). Later, in mid-oogenesis, β_H is slightly enriched on the outer edge of the ring canals (Fig. 1 F).

In the soma, β_H is strongly expressed at the very anterior tip of the germarium in the terminal filament and the cap cells that contact the germline stem cells (Fig. 1, A and B). In close proximity to the 16 cell cysts in region 2, we detect high levels of β_H expression in the vicinity of the somatic stem cells and in their progeny, the follicle cells (Fig. 1, A and B). As individual cysts become enveloped in follicle cells, β_H is slightly enriched in the cells that move in to segregate adjacent cysts (Fig. 1 B). β_H continues to be strongly expressed here as these become the stalk cells that separate successive egg chambers along the ovariole (Fig. 1 A, arrow). β_H is apically polarized in the follicle cells (Fig. 1, A and B). β_H is downregulated in the migrating border cells at stage 9 (Fig. 1 A, *), but is again expressed on the apical surface of these cells when they begin to secrete the micropyle after stage 10 (Fig. 1, C and E, arrowheads). At stage 10, β_H is part of a prominent terminal web-like structure at the apical ends of the follicle cells that are secreting egg components (Fig. 1 G). This structure appears to be anchored in the ZA by fine fibers of staining around its edge. β_H is also expressed on the apical surfaces of the follicle cells secreting the dorsal appendages (Fig. 1 D, arrow) and the chorion (data not shown). β_H colocalizes with α-spectrin in the germline and soma at all these locations (Fig. 1); however, the latter is more widespread presumably through its association with the conventional β isoform.

Border and Follicle Cell Migrations Are Uncoordinated in karst Mutant Egg Chambers

In mid–stage 9 egg chambers, the follicle cell monolayer and the border cells migrate in a concerted fashion (Mon-

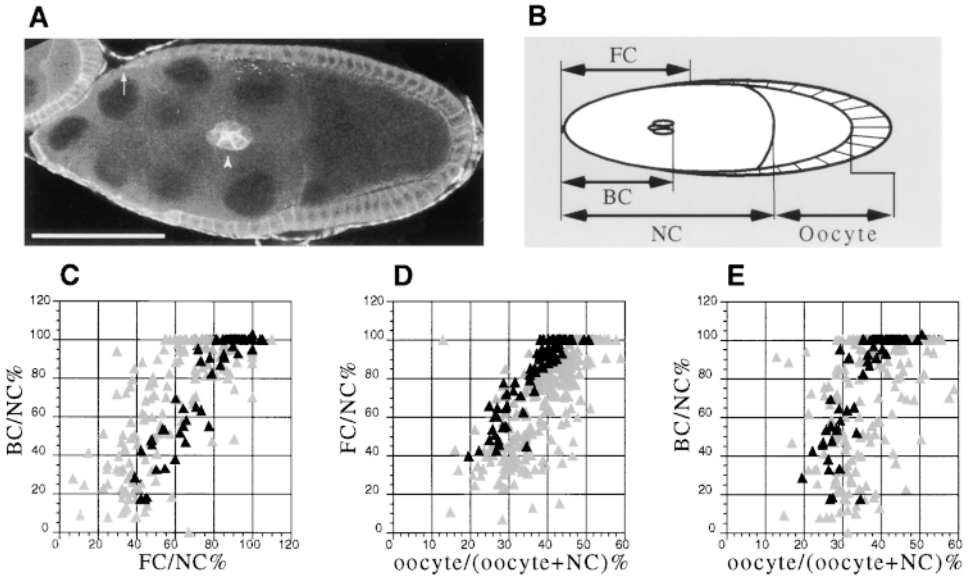

Figure 2. Morphometric analysis of *karst* mutant egg chambers. (A) A stage 9 *karst* mutant egg chamber stained for α-spectrin. Note the border cell cluster (arrowhead) is migrating ahead of the trailing edge of the follicle cell monolayer (arrow). Scale bar, 50 μm. (B) Schematic diagram of a stage 9 egg chamber and the parameters measured: (FC) Distance between the anterior tip of the egg chamber and the trailing edge of the migrating follicle cell monolayer, (BC) distance between the anterior tip of the egg chamber and the leading edge of the border cell cluster, (NC) nurse cell cluster length, (Oocyte) oocyte length. All measurements were done on the anterior–posterior axis in sagittal confocal sections. (C–E) Pairwise comparisons of FC, BC, and Oocyte measured as shown in B and normalized against NC, which remains constant during this stage. Measurements from 81 wild-type chambers are plotted with black symbols, data from 318 *karst* mutant egg chambers are shown in gray.

tell et al., 1992; see also Fig. 1). However, in 73% of *karst* egg chambers the border cells migrate ahead of the follicle cell monolayer (Fig. 2 A). The degree to which the border cells migrate ahead of the follicle cells during stage 9 is quite variable in keeping with the variable expressivity of the *karst* mutation (Thomas et al., 1998). We occasionally find egg chambers where the border cells are retarded relative to the follicle cells; however, this extreme situation probably arises from a combination of weak expression of the follicle cell phenotype combined with strong expression of the border cell phenotype (see Discussion).

The lack of coordination in cell migration makes it difficult to assess the progression of each chamber through stage 9. We therefore resorted to a morphometric approach. The four distances indicated in Fig. 2 B were measured in sagittal optical sections of 81 wild-type and 318 *karst* mutant egg chambers. Since the nurse cells do not grow or shrink at this time, all these measurements were normalized against the anterior-posterior length of this cell cluster.

Pairwise comparisons of the parameters (FC/NC), (BC/NC), and [oocyte/(oocyte+NC)] (Fig. 2, C–E) reveals the following defects in *karst* mutant egg chamber morphogenesis. (a) Most *karst* border cell clusters are migrating ahead of the follicle cell monolayer during stage 9 (Fig. 2 C). This could arise either due to faster border cell migration or slower follicle cell migration. (b) Most *karst* mutant oocytes occupy a larger portion of the egg chamber than in the wild-type during follicle cell migration, while the oocyte exhibits no significant overgrowth at the completion of migration (Fig. 2 D). This suggests that *karst* follicle cells are delayed in their migration relative to growth of the oocyte, or may respond more slowly to oocyte growth. (c) Similarly, most *karst* mutant oocytes occupy a larger portion of the egg chamber than in wild-type during border cell migration (Fig. 2 E). This effect is not as strong as for the follicle cells, consistent with the observation that the border cells generally migrate ahead of the follicle cells in *karst* mutant egg chambers, but it does suggest that there is a slight delay in border cell migration. The most parsimonious model accounting for these data suggests that the *karst* mutation causes a significant disruption of follicle migration onto the oocyte membrane and a slight delay in border cell delamination or migration through the nurse cells.

Consistent with the hypothesis that the primary morphogenetic defect lies in follicle cell migration, some follicle cells in *karst* mutant egg chambers often remain in contact with the nurse cell membranes at stage 10A. These follicle cells still attempt to make the appropriate adhesive contacts with the oocyte membrane (Goode et al., 1996), pulling the oocyte membrane towards them and grossly distorting the nurse cells/oocyte interface (Fig. 3 A). In most cases, the subsequent inward migration of the follicle cell layer at stage 10B proceeds along the nurse cell/oocyte interface in a relatively normal fashion. However, in rare, extreme cases, the centripetally migrating cells penetrate between nearby nurse cell membranes and cause one or more nurse cells to become included within the egg along with the oocyte (Fig. 3 B).

Aberrant Follicle Cell Migration Results from a Failure in Apical Constriction

The failure of *karst* follicle cells to complete their migration onto the oocyte by the onset of stage 10B implies that the total apical surface area of the epithelium is greater than that of the oocyte membrane. Moreover, *karst* mutant follicle cells often appear to have a more cuboidal shape than in the wild-type (see Fig. 5, G and H). Since

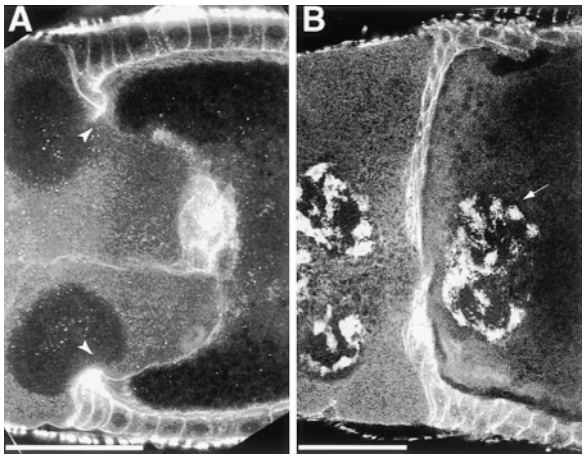

Figure 3. Oocyte distortion and centripetal cell migration defects in *karst* mutant egg chambers. (A) Midregion of a sagittal section through a stage 10A-B *karst* mutant egg chamber costained for actin and *D*E-cadherin. Note the distorted interface between nurse cells and oocyte (between arrowheads). (B) Midregion of a stage 10B *karst* mutant egg chamber costained for α-spectrin and propidium iodide. In this severe case, the centripetal cells of the incompletely migrated follicle cell layer have disrupted the nurse cell cluster and incorporated a nurse cell nucleus (arrow) into the oocyte. Both channels were flattened into a grayscale image in each panel. Anterior is to the left in both panels. Scale bars, 50 μm.

there is no over-proliferation in the mutant monolayer (data not shown), this cannot arise due to an increase in cell number. However, an inability of *karst* follicle cells to properly change their cell shape or constrain their apical surface area at the appropriate size would explain this observation. We therefore compared the apical surface area of wild-type and mutant follicle cells during monolayer migration. This analysis reveals a sharp decrease in the apical surface area of the wild-type follicle cells as they approach and migrate onto the oocyte (Fig. 4 A). In contrast, the majority of *karst* mutant follicle cells fail to apically constrict (Fig. 4 A). The mean apical surface area of the mutant follicle cells is almost twice that of the wild-type (Fig. 4 B). Moreover, comparison of the apical surface areas of mutant follicle cells in chambers during migration with those where migration has been completed reveals a slight increase (Table I; $P < 0.001$). This suggests that, in addition to the constriction defect, the monolayer cannot withstand the forces exerted by the growing oocyte.

The zonula adherens Is Disrupted in karst Mutant Follicle Cells

Examination of the follicle cell apices stained for *D*E-cadherin also reveals conspicuous disruptions in the staining pattern of *D*E-cadherin in *karst* mutant egg chambers (Fig. 5, A–F). In the mildest cases, this staining is missing at three- or four-cell vertices, but we also see large breaks in the normally continuous belt of staining in more extreme cases. These observations are consistent with the hypothesis that the absence of β_H weakens the ZA, and that it breaks up as the apices attempt to constrict or accommodate the growth of the oocyte. However, the apicolateral polarization of the ZA is largely unaffected (Fig. 5, G and H).

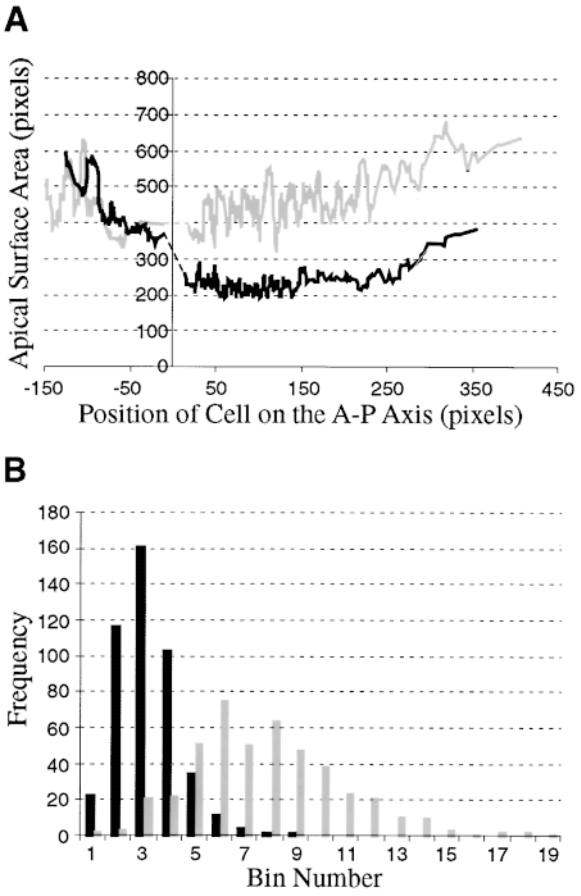

Figure 4. karst follicle cells fail to constrict their apices over the oocyte. (A) Plot of 578 wild-type apical cell areas from 17 egg chambers (black line) and 603 *karst* mutant apical cell areas from 19 egg chambers (gray line) versus each cell's position on the anterior–posterior axis. The origin of the x axis corresponds to the boundary between the nurse cell cluster and the oocyte. Each line is a rolling average (window size = 10 pixels). (B) Histograms representing the distribution of apical surface areas from those follicle cells residing on the oocyte. Data was grouped as follows: bin 1 = 0–50 pixels, bin 2 = 51–100 pixels, bin 3 = 101–150 pixels, etc., up to bin 19 = 901–950 pixels.

The Border Cell Cluster is Often Disrupted in karst Mutants

The border cell cluster delaminates from the follicle cell epithelium and migrates between the nurse cells to the an-

Table I. Wild-type and karst Follicle Cell Apical Surface Areas during and after Migration

	Surface area of cells over the oocyte (pixels±SD)	
Stage	Wild-type	*karst*
9	234.1±61.3	435.9±149.6
	n = 201 cells from 8 chambers	n = 287 cells from 11 chambers
10A	236.5±66.9	504.4±151.6
	n = 259 cells from 8 chambers	n = 169 cells from 8 chambers

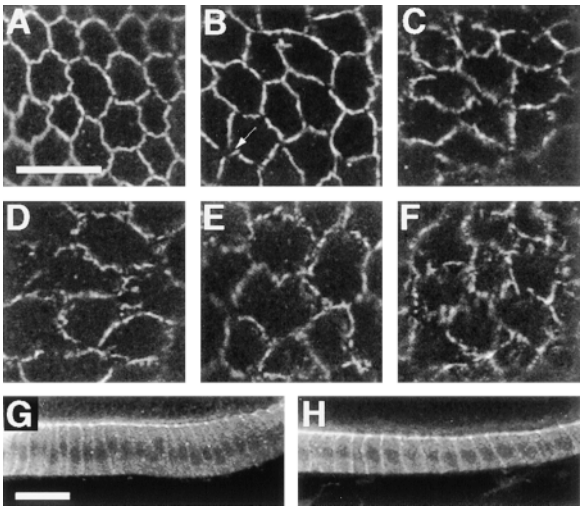

Figure 5. The *zonula adherens* is severely disrupted and cell shape is affected in *karst* mutant follicle cells covering the oocyte. (A–F) Confocal sections at the apical surface showing *D*E-cadherin immunolocalization at the ZA in stage 9/10A wild-type (A) and *karst* mutant (B–F) follicle cells. B–F represent the different degrees of phenotypic severity seen in mutant cells. In the mildest case, disruption of the ZA is most apparent at the vertex between three and four cells (B, arrow). (G and H) Confocal cross-sections of follicle cells showing *D*E-cadherin immunolocalization in stage 9/10A wild-type (G) and *karst* mutant (H) follicle cells. *karst* mutant cells with enlarged apices are more cuboidal than in wild type. Scale bar in A represents 10 μm and applies to A–F. Scale bar in G represents 20 μm and applies to G and H.

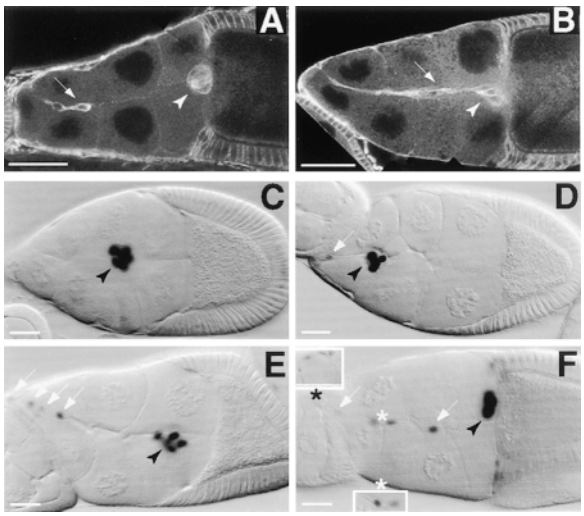

Figure 6. Border cell clusters are disrupted in *karst* mutant egg chambers. (A and B) Sagittal confocal sections of stage 10A and B mutant egg chambers stained for α-spectrin. Cells separated from the main border cell cluster (arrowheads) migrate either separately (A, arrow) or in a trail (B, arrow). All cells migrating between nurse cell membranes in *karst* mutant egg chambers express *slbo*. (C) β-Galactosidase activity staining marks the border cell cluster (black arrowhead) in $slbo^1$/+ marked wild-type ovaries. (D–F) All cells migrating between the nurse cells in $slbo^1$/+; *kst* ovaries, including the main border cell cluster (black arrowhead) and the separated cells (white arrows), express *slbo*. White asterisks indicate cells slightly off the focal plane that are shown again in focus in the corresponding marked insets. Insets marked with black asterisks show staining cells completely out of the main focal plane. All chambers are at stage 9 or 10A. β-Galactosidase activity staining was performed simultaneously with DAPI nuclear staining to ensure that all cells penetrating the nurse cell cluster were identified (data not shown). Scale bar represents 50 μm in A and B, 10 μm in D–F.

terior of the oocyte during stage 9. In ~10% of *karst* mutant egg chambers, we observe migratory cells that are well separated from, or trail behind, the main border cell cluster (Fig. 6). The trailing cells upregulate α-spectrin (Fig. 6, A and B) and *D*E-cadherin (data not shown) in a manner that resembles wild-type clusters, suggesting that they are true border cells. To confirm that these cells have a border cell fate, we looked for the expression of the border cell marker *slow border cells* (*slbo*) by introducing the enhancer trapped *LacZ* gene associated with the $slbo^1$ P-element allele (Montell et al., 1992) into the *karst* mutant background and staining for β-galactosidase activity. All of the migratory cells in $slbo^1$/+; *kst* egg chambers express β-galactosidase, although the intensity of staining exhibited by the separated cells is often lower than the main border cell cluster (Fig. 6, D–F). None of the trailing cells express Fasciclin III, indicating that they do not contain polar cells (data not shown; Patel et al., 1987), and thus do not represent second, independently organized, migratory clusters. Furthermore, the total number of β-galactosidase–positive cells ranges from 7 to 11, very close to the normal range in border cell number in wild-type chambers (6–10; Spradling, 1993). Together, these data suggest that all of the migratory cells are bona fide border cells and that the normal number of border cells is specified in *karst* mutants, but that the cluster is unable to remain together as a unit.

The Apical Spectrin Membrane Skeleton Is Absent in karst Mutant Follicle Cells

β_H is no longer detectable at the apical domain of the follicle cells in any allelic combination of *karst* alleles that we have examined (data not shown). The localization of β_H to the apical domain has been previously shown to be dependent on α-spectrin (Lee et al., 1997). To see if α-spectrin is dependent on β_H for its localization to the apical domain, and to confirm that no apical spectrin function remains in *karst* mutants, we examined the distribution of α-spectrin in *karst* follicle cells. While the lateral α-spectrin distribution is unaffected by this mutation, apical α-spectrin is no longer detectable by immunofluorescence (Fig. 7, C and E). This indicates that the stable recruitment of α-spectrin to the apical domain is dependent on β_H, and that there is thus a mutual interdependence between α-spectrin and β_H. This further suggests that $\alpha\beta_H$-spectrin is recruited to the apical domain as a heterodimer or tetramer, or that following separate recruitment only the dimers or tetramers remain stably associated with the apical domain.

Apicobasal Polarity Is Maintained in karst Mutant Follicle Cells

Spectrin associated with E-cadherin has been implicated

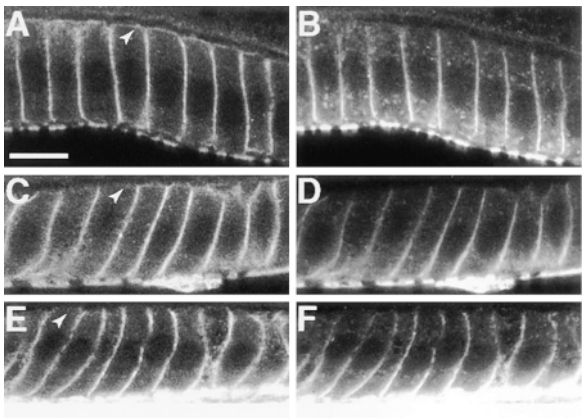

Figure 7. β_H is required for a stable spectrin membrane skeleton in the apical domain. Part of three follicle cell monolayers co-stained for α-spectrin (A, C, and E) and β-spectrin (B, D, and F) are shown. (A and B) Wild-type follicle cell monolayer. Arrowhead indicates an example of α-spectrin in the apical domain. Both α- and β-spectrins stain the lateral membranes. (C–F) two examples of *karst* mutant follicle cell monolayers (*kst*^{01318} in C and D, *kst*^{2}*/Df(3L)1226* in E and F). α-Spectrin is no longer present at the apical membrane domain (C and E, arrowheads), and there is no change in the distribution of β-spectrin in any allelic combination (D and F). Scale bar represents 10 μm. The strong staining on the basal side of the epithelia corresponds to the surrounding muscle sheath.

in the apicobasal cell polarization pathway (Yeaman et al., 1999), and fly α-spectrin mutations cause a breakdown in monolayer polarity including the loss of apical β_H (Lee et al., 1997). However, *karst* mutants form a follicle epithelium that appears to have a well polarized morphology. To further verify this observation, we examined the distribution of the apical markers Notch, myosin II, and unconventional myosin IB (data not shown; Edwards and Kiehart, 1996; Morgan et al., 1995; Xu et al., 1992), as well as the apical concentration of actin in the follicle cell brush border. These and similar experiments in mutant eye and wing imaginal discs (data not shown) indicate that the distribution of several apical markers is not conspicuously affected by the lack of β_H.

Given the significant similarity between β_H and β-spectrin (Thomas et al., 1997), it is also possible that polarity is retained in *karst* mutant epithelia because of functional redundancy between these two proteins. Moreover, the *karst* mutant phenotype exhibits variable expressivity despite genetic evidence that we have null alleles (Thomas et al., 1998), and this might also result from functional redundancy. Such redundancy would predict that conventional β-spectrin would be recruited to the apical domain in the absence of β_H. However, this is not the case (Fig. 7, B, D, and F), confirming that β_H is unnecessary for apicobasal polarity and indicating that we must look elsewhere for the source of variability in the *karst* phenotype.

Discussion

β_{Heavy}-spectrin is a member of the spectrin family of proteins that have been implicated in cadherin-mediated cell polarization (Yeaman et al., 1999), and is associated with the ZA (Thomas et al., 1998; Thomas and Williams, 1999). In this paper, we have characterized the effects of loss of function *karst* mutations (which eliminate β_H) on fly oogenesis. These mutations cause defects in the migration of the follicle cell monolayer and in border cell delamination, but do not compromise the apicobasal polarity of its constituent cells. The defect in monolayer migration is characterized by a failure of the follicle cells to constrict their apical surfaces and by visible breaks in the ZA.

β_H Is Polarized in Somatic Epithelia but Not in Germline Cells

We present here the first complete description of the distribution of β_H during *Drosophila* oogenesis (Fig. 1). β_H is strongly expressed in the terminal filaments and cap cells that sit adjacent to the germline stem cells at the anterior end of the germarium. In the germline, it is first seen on the membrane in region 2, in the 8–16-cell cysts. β_H is not obviously polarized at any of these locations, and remains uniformly distributed in the nurse cells and oocyte. In the soma, β_H is prominently expressed in the vicinity of the somatic stem cells and their derivative, the follicle cell epithelium, where it is restricted to the apical domain. These results corroborate the previous partial descriptions of the distribution of β_H during oogenesis (de Cuevas et al., 1996; Lee et al., 1997). We have also found that β_H is prominently expressed in the stalk cells, at a number of sites of high secretory activity late in oogenesis, and is downregulated in the border cells during their migration.

The downregulation of β_H in the anterior region of the germarium would suggest that β_H has no role in germ cell division and/or oocyte specification within the germline. However, β_H is strongly expressed in the terminal filament and cap cells that sit adjacent to the germline stem cells and early cystoblasts, the cellular activities of which are believed to regulate germline stem cell division and polarization (reviewed in Spradling et al., 1997). β_H could thus interact with one or more components in the terminal filament and cap cells to generate signals that affect polarity or proliferation in the germline.

β_H is part of a prominent terminal web subtending the follicle cell brush border that forms as they migrate onto the oocyte at stage 9 and begin to secrete yolk protein. β_H is also expressed in the border cells once these cells begin to secrete the micropyle and in the follicle cells that are secreting chorion to form the dorsal appendages. The prominence of β_H in all these locations of high secretory activity suggests that there may be a role for the apical membrane skeleton in the targeting or delivery of secretory vesicles even though it is not required for overall apicobasal polarity (see below). A similar role has been proposed for the gut-specific terminal web β-spectrin, TW260, in the chicken (Hirokawa et al., 1983).

β_{Heavy}-Spectrin Is Required for Epithelial Morphogenesis

In *karst* mutant ovaries, the primary defect in follicle cell morphogenesis is a failure of this monolayer to complete migration onto the oocyte membrane by the end of stage 9 (Figs. 2 and 3). Specifically, these cells fail to undergo the

normal apical contraction associated with the development of a more columnar shape upon contacting the oocyte membrane (Fig. 4). Furthermore, staining for the ZA marker *D*E-cadherin revealed conspicuous breaks in the normally continuous belt of staining for this protein around the follicle cell apices (Fig. 5).

Apical contraction is a well established process for the generation of form in an epithelium; however, the exact mechanism by which cells achieve this phenomenon is still unclear. β_H is associated with two actin-rich structures at the apical pole, the ZA and the terminal web subtending the microvillar brush border. F-actin at the ZA lies in a circumferential band of microfilaments of mixed orientation that can be induced to undergo a purse string–like contraction in vitro that is mediated by myosin II (Burgess, 1982; Hirokawa et al., 1983; Keller et al., 1985). β_H may be necessary for contraction of this bundle. Spectrin cross-linking of F-actin can stimulate myosin ATPase (Coleman and Mooseker, 1985) and is necessary for cortical contraction of sea urchin eggs (Walker et al., 1994). The distribution of myosin II was not conspicuously affected in *karst* mutant follicle monolayers (data not shown); however, β_H may be necessary for the correct organization of the contractile actin bundle through its ability to cross-link F-actin, or for the attachment of the bundle to the membrane or the ZA.

Alternatively, β_H may play a structural role in the follicle cell terminal web (Mahowald, 1972; Morgan et al., 1995). This is a region of dense actin cross-linking between bundles of microfilaments that support the overlying microvilli and is integrated into the circumferential F-actin bundle and the ZA at its margins. This structure also contains myosin II (Herman and Pollard, 1981; Hirokawa et al., 1982), but is not contractile. However, a decrease in apical surface area presumably requires remodeling of the terminal web to produce a corresponding decrease in the size of this network or an increase in microvillar density. Neither a terminal web nor β_H is required to produce microvilli (Fath and Burgess, 1995; Thomas et al., 1998). However, β_H in the terminal web might help stabilize the contractile process. The apical domain of all of the follicle cells must apically constrict, presumably generating significant tension in the adhesive network that binds the epithelium together. In this particular case, the terminal web may be an essential structural component of a supracellular actin network. The lack of cross-linking by β_H in the terminal web might thus result in excessive strain on the ZA and its ultimate breakage.

The fact that follicle cell migration does initiate and proceed to some extent in *karst* mutants indicates that not all motile forces are eliminated by this mutation. This may simply mean that not all intercellular tension generated by apical constriction is eliminated by the *karst* mutation. However, another possibility is that apical constriction is not the only force-generating mechanism responsible for monolayer migration. Indeed, the observation that hypomorphic mutations in the regulatory light chain of cytoplasmic myosin II do not prevent the migration of the follicle cell monolayer (Edwards and Kiehart, 1996) does indicate this. At least two other forces should be considered. First, the oocyte is growing through the uptake of hemolymph and yolk during stage 9, and this inflation may contribute to migration and to tension at the ZA. Second, the follicle cells make specific adhesive contact with the oocyte membrane (Goode et al., 1996) and this might produce localized tension as each follicle cell first contacts, and then moves onto the oocyte.

The failure of *karst* follicle cells to complete their migration onto the oocyte by the onset of stage 10B leads to aberrant centripetal cell migration in a small number of egg chambers. In such cases, the inwardly migrating cells find their way in between nurse cell membranes enclosing one of the latter along with the oocyte. Given the high frequency of defective migration, it is perhaps surprising that this latter defect is relatively rare and that oogenesis can often proceed to completion in the absence of β_H. We suspect that the ability of the centripetally migrating cells to seek out the nurse cell/oocyte interface by specific adhesion to the oocyte membrane (Goode et al., 1996) results in a substantial compensation for the migration defect that is generated by the *karst* mutation. Thus, the inclusion of a nurse cell with the oocyte after centripetal cell migration is infrequent and a relatively normal egg results. Moreover, after migration is completed, the oocyte continues to grow as dumping occurs and the egg matures, during which time the follicle cell apices must again grow and presumably any slack in the *karst* monolayer is taken up. This would explain why *karst* mutant females are not completely sterile and do lay some fertilized eggs.

β_{Heavy}-Spectrin Is Required for Border Cell Morphogenesis

The border cells delaminate from the follicular epithelium at the onset of stage 9 and migrate between the nurse cells to the anterior of the oocyte (Spradling, 1993). As part of this developmental program, we have shown that they downregulate β_H. While there is no detectable β_H at any of the border cell–border cell interfaces, it is difficult to say with certainty that there is no β_H in a normal cluster. This is because these cells do not fully depolarize (Niewiadomska et al., 1999), and the residual apical surface is closely juxtaposed to the surrounding nurse cell membranes that contain abundant β_H protein. Migration normally occurs as a tight cluster of 6–10 cells; however, in *karst* mutant egg chambers, one or more border cells are separated from the main cluster (Fig. 6).

The presence of β_H at two or possibly three locations during normal border cell delamination and migration suggests a number of possible roles for this protein in border cell morphogenesis. Its presence at the nurse cell membranes on which the border cells migrate could contribute to the rigidity of this substratum or to inter-nurse cell adhesion. In this context, we note the similarity between the patchy distribution of β_H (Fig. 1 A, arrowhead) along the border cell migration route and that of *D*E-cadherin, a molecule required for migration (Oda et al., 1997; Niewiadomska et al., 1999). The loss of either of these functions might impact border cell migration. β_H might also be present on the outermost apical surface of the migrating border cell cluster. Here it could contribute to the adhesion between the border cells and the nurse cells. Loss of this function might cause the border cell cluster to have difficulty attaching to the nurse cells during delamination and the subsequent migration. Finally, β_H is

present in the nonmigratory follicle cells that surround the delaminating cluster, where it might play a role in border cell delamination. This latter hypothesis is the most likely explanation for the border cell phenotype. If the absence of β_H either on the apical border cell surface or on the nurse cell surface was responsible for the breakup of the cluster, we would expect to see either a more dramatic or a preferential breakup of clusters late in migration. However, there is no indication that the number of separated cells increases with the distance migrated and we see many examples of early break up.

The normal boundary between the border cells that will delaminate and the surrounding follicle cells is marked by a dramatic decrease in the level of β_H in the border cells. In addition, β_H is also prominent at the follicle cell/border cell membrane interface during delamination. This boundary must have at least two properties. It must serve to allow the border cells to detach and it must allow the follicle cell monolayer to reseal the gap left by the departing cluster. We hypothesize that the presence of β_H in the surrounding follicle cells is part of a differential adhesion system that causes the surrounding, nonmigratory follicle cells to seek out one another to reseal the gap and in doing so to sacrifice contact with the border cells. Elimination of β_H in the nonmigrating cells would affect the precise physical boundary between groups of cells with different adhesive properties preventing this rearrangement of cell contacts, and thus proper detachment of the border cells. The precise role of β_H in generating this boundary remains open. β_H is localized in part at the ZA and its presence or absence could be responsible for modulating *D*E-cadherin–based adhesion. Such differential adhesion is clearly part of the mechanism by which the oocyte positions itself relative to the overlying follicle cells (Godt and Tepass, 1998; Gonzalez-Reyes and St. Johnston, 1998). However, such sharp transitions in cell fate can be generated by lateral inhibition mechanisms (Artavanis-Tsakonas et al., 1999), and it is also possible that β_H is responsible for stabilizing some of the signaling molecules involved in such processes during border cell specification.

Apicobasal Polarity Does Not Require Apical Spectrin

The initial development of the follicular epithelium is essentially unaffected by the loss of either α-spectrin (Deng et al., 1995; Lee et al., 1997) or β_H (this paper), suggesting that the spectrin membrane skeleton is not essential for the establishment of polarity in this particular case. We have also demonstrated that there is no conspicuous breakdown of apicobasal polarity in the absence of the apical SBMS later in oogenesis (Fig. 7). This contrasts with the phenotype of α-spectrin mutants in *Drosophila* (Deng et al., 1995; Lee et al., 1997), in which a loss of cell polarity and breakdown of the follicular epithelium is seen. Together, these two results indicate that the loss of apicobasal polarity in the α-spectrin mutants reflects a requirement for the basolateral SBMS specifically, or is a synergistic consequence of losing both the apical and basolateral membrane skeletons. Resolution of this ambiguity awaits further characterization of β-spectrin mutants. Although overall apicobasal polarity remains intact in *karst* mutants, it remains possible that specific proteins that are dependent on binding to the apical SBMS for delivery and/or retention in the apical membrane are depolarized by the absence of $(\alpha\beta_H)_2$.

In keeping with the observation that different spectrin isoforms do not generally colocalize (Glenney and Glenney, 1983; Lazarides et al., 1984), β_H and β-spectrin are found in mutually exclusive domains in epithelial tissues (Dubreuil et al., 1997, 1998; Lee et al., 1997; Thomas et al., 1998). β-spectrin is recruited to the membrane by proteins that bind to the adapter protein ankyrin (Dubreuil et al., 1997). However, β_H lacks an ankyrin binding site and is not recruited in this manner (Dubreuil et al., 1997; Lee et al., 1997; Thomas et al., 1997). Integral membrane proteins that bind to ankyrin thus provide a polarizing influence that can specifically establish a basolateral membrane skeleton. In this paper, we have shown that in the absence of β_H, β-spectrin does not become recruited to the apical surface. This indicates that β_H is not excluding β-spectrin from potential binding sites in this domain and that β_H must therefore be specifically recruited to this domain. This result is also significant because it implies that the variable expressivity associated with the *karst* phenotype (Thomas et al., 1998) does not arise through redundancy of function between β_H and β-spectrin.

Current models for the origins of epithelial polarity suggest that spectrin plays a key role in establishing and/or maintaining the apicobasal axis (Yeaman et al., 1999). This model is largely based on the behavior of molecules involved in establishing the basolateral domain. The combined observations on the α-spectrin (Deng et al., 1995; Lee et al., 1997) and *karst* mutant phenotypes suggests that the basolateral membrane skeleton may be playing such a role; however, our results indicate that apical spectrin [i.e., $(\alpha\beta_H)_2$] does not. It remains unclear what the precise mechanism is by which apical spectrin acts during morphogenetic events. β_H exhibits a close colocalization with the ZA, and its levels at this location are regulated in concert with *D*E-cadherin (Thomas et al., 1998; Thomas and Williams, 1999). Furthermore, we have observed mild disruptions of the ZA in eye/antennal imaginal discs (Zarnescu, D.C., and G.H. Thomas, unpublished observations) that are similar to the effects reported in this paper. None of our results to date reveal how closely $(\alpha\beta_H)_2$ is associated with the ZA; however, the contrasting behavior of the apical and basolateral SBMS during the emergence of apicobasal polarity (Thomas and Williams, 1999) combined with the phenotypic data presented in this paper strongly suggest that these two cytoskeletal structures have somewhat distinct rather than identical roles in their respective domains, at least when it comes to the generation and/or maintenance of apicobasal polarity.

Conclusions and Perspective

The results presented in this paper add to a growing body of evidence that apical spectrin is essential for epithelial morphogenesis. Moreover, we show that an apical SBMS is not required for establishing or maintaining apicobasal polarity, as seems to be the case for the basolateral SBMS. It is unknown at present whether or not β_H or any other β-spectrin plays a similar role in morphogenesis in vertebrates. The observations that β_H is evolutionarily old

(Thomas et al., 1997), that there is a homologue in *C. elegans* encoded by the *sma1* gene (McKeown et al., 1998), and that the chicken brush border protein TW260 has a similar size and contour length to β_H (350 kD; Dubreuil et al., 1990; Glenney et al., 1982), all strongly suggest that there is a vertebrate homologue of β_H that has yet to be cloned. The *karst* phenotype bears close resemblance to the phenotype exhibited by *C. elegans* embryos mutant at the *sma1* locus that encodes the worm homologue of β_H (McKeown et al., 1998). In *sma1* mutants, the worms fail to elongate at the wild-type rate during embryogenesis, resulting in a smaller embryo. Moreover, this phenotype seems to arise from a defective contraction of the embryonic epithelium (McKeown et al., 1998). Thus, while the geometry of this developmental event is quite different from follicle cell migration in the fly, β_H appears to be playing a similar role in the two organisms. In vertebrates, the apical accumulation of spectrin has been correlated with the initiation of neurulation in mice (Sadler et al., 1986), and, in the sea urchin embryo, an apical accumulation of α-spectrin is associated with the involution of tissues during embryogenesis (Wessel and Chen, 1993). This suggests that apical spectrin has a general role in the morphogenesis of epithelia mediated by apical contraction.

The authors thank Spyros Artavanis-Tsakonas, Dan Branton, Dan Kiehart, John Lee, Mark Mooseker, and Tadashi Uemura for gifts of antibodies, Denise Montell for supplying the *slbo*^{1} enhancer trap line, and Carol Gay for the use of her confocal microscope. We also thank Maggie de Cuevas and Bryce MacIver for useful discussions, as well as Susan Abmayr, Esther Siegfried, and the members of the Thomas lab for critically reading this manuscript.

This work was funded by National Institutes of Health grant GM52506 to G.H. Thomas.

Submitted: 10 June 1999
Revised: 4 August 1999
Accepted: 5 August 1999

References

Artavanis-Tsakonas, S., M.D. Rand, and R.J. Lake. 1999. Notch signaling: cell fate control and signal integration in development. *Science*. 284:770–776.

Beck, K.A., J.A. Buchanan, V. Malhotra, and W.J. Nelson. 1994. Golgi spectrin: identification of an erythroid β-spectrin homolog associated with the golgi complex. *J. Cell Biol.* 127:707–723.

Bennett, V., and D.M. Gilligan. 1993. The spectrin-based membrane skeleton and micron-scale organization of the plasma membrane. *Annu. Rev. Cell Biol.* 9:27–66.

Burgess, D.R. 1982. Reactivation of intestinal epithelial cell brush border motility: ATP-dependent contraction via a terminal web contractile ring. *J. Cell Biol.* 95:853–863.

Byers, T.J., E. Brandin, R.A. Lue, E. Winograd, and D. Branton. 1992. The complete sequence of *Drosophila* beta-spectrin reveals supra-motifs comprising eight 106-residue segments. *Proc. Natl. Acad. Sci. USA*. 89:6187–6191.

Byers, T.J., R. Dubreuil, D. Branton, D.P. Kiehart, and L.S.B. Goldstein. 1987. *Drosophila* spectrin. II. Conserved features of the alpha-subunit are revealed by analysis of cDNA clones and fusion proteins. *J. Cell Biol.* 105: 2103–2110.

Byers, T.J., A. Husain-Chisti, R.R. Dubreuil, D. Branton, and L.S.B. Goldstein. 1989. Sequence similarity of the amino-terminal domain of *Drosophila* beta spectrin to alpha actinin and dystrophin. *J. Cell Biol.* 109:1633–1641.

Cohen, C., and P. Gascard. 1992. Regulation and post-translational modification of erythrocyte membrane and membrane-skeletal proteins. *Semin. Hematol.* 29:244–292.

Coleman, T.R., and M.S. Mooseker. 1985. Effects of actin filament cross-linking and filament length on actin-myosin interaction. *J. Cell Biol.* 101:1850–1857.

de Cuevas, M., J.K. Lee, and A.C. Spradling. 1996. α-Spectrin is required for germline cell division and differentiation in the *Drosophila* ovary. *Development (Camb.)*. 122:3959–3968.

DeMatteis, M.A., and J.S. Morrow. 1998. The role of ankyrin and spectrin in membrane transport and domain formation. *Curr. Opin. Cell Biol.* 10:542–549.

Deng, H., J.K. Lee, L.S.B. Goldstein, and D. Branton. 1995. *Drosophila* development requires spectrin network formation. *J. Cell Biol.* 128:71–79.

Dubreuil, R.R., T.J. Byers, C.T. Stewart, and D.P. Kiehart. 1990. A β-spectrin isoform from *Drosophila* (β_H) is similar in size to vertebrate dystrophin. *J. Cell Biol.* 111:1849–1858.

Dubreuil, R.R., J. Frankel, P. Wang, J. Howrylak, M. Kappil, and T.A. Grushko. 1998. Mutations of alpha spectrin and labial block cuprophilic cell differentiation and acid secretion in the middle midgut of *Drosophila* larvae. *Dev. Biol.* 194:1–11.

Dubreuil, R.R., P.B. Maddux, T.A. Grushko, and G.R. MacVicar. 1997. Segregation of two spectrin isoforms: polarized membrane-binding sites direct polarized membrane skeleton assembly. *Mol. Biol. Cell*. 8:1933–1942.

Edwards, K.A., and D.P. Kiehart. 1996. *Drosophila* nonmuscle myosin II has multiple essential roles in imaginal discs and egg chamber morphogenesis. *Development (Camb.)*. 122:1499–1511.

Fath, K.R., and D.R. Burgess. 1995. Not actin alone. *Curr. Biol.* 5:591–593.

Freeman, M., C. Nusslein-Volhard, and D.M. Glover. 1986. The dissociation of nuclear and centrosomal division in *gnu*, a mutation causing giant nuclei in *Drosophila*. *Cell*. 46:457–468.

Glenney, J.R., Jr., and P. Glenney. 1983. Fodrin is the general spectrin-like protein found in most cells whereas spectrin and the TW protein have restricted distribution. *Cell*. 34:503–512.

Glenney, J.R., Jr., P. Glenney, M. Osborn, and K. Weber. 1982. An F-actin– and calmodulin-binding protein from isolated intestinal brush borders has a morphology related to spectrin. *Cell*. 28:843–854.

Godt, D., and U. Tepass. 1998. *Drosophila* oocyte localization is mediated by differential cadherin-based adhesion. *Nature*. 395:387–391.

Gonzalez-Reyes, A., and D. St. Johnston. 1998. The *Drosophila* AP axis is polarised by the cadherin-mediated positioning of the oocyte. *Development (Camb.)*. 125:3635–3644.

Goode, S., M. Melnick, T.-B. Chou, and N. Perrimon. 1996. The neurogenic genes *egghead* and *brainiac* define a novel signaling pathway essential for epithelial morphogenesis during *Drosophila* oogenesis. *Development (Camb.)*. 122:3863–3879.

Gumbiner, B.M. 1992. Epithelial Morphogenesis. *Cell*. 69:385–387.

Gumbiner, B.M. 1996. Cell adhesion: basis of tissue architecture and morphogenesis. *Cell*. 84:345–357.

Hammerton, R.W., K.A. Krzeminski, R.W. Mays, T.A. Ryan, D.A. Wollner, and J.W. Nelson. 1991. Mechanism for regulating cell surface distribution of Na^+, K^+-ATPase in polarized epithelial cells. *Science*. 254:847–850.

Herman, I., and T.D. Pollard. 1981. Electron microscopic localization of cytoplasmic myosin with ferritin-labeled antibodies. *J. Cell Biol.* 88:346–351.

Hirokawa, N., T.C.S. Keller III, R. Chasan, and M.S. Mooseker. 1983. Mechanism of brush border contractility studied by the quick-freeze, deep-etch method. *J. Cell Biol.* 96:1325–1336.

Hirokawa, N., L.G. Tilney, K. Fujiwara, and J.E. Heuser. 1982. The organization of actin, myosin and intermediate filaments, in the brush border of intestinal epithelial cells. *J. Cell Biol.* 94:425–443.

Holleran, E.A., M.K. Tokito, S. Karki, and E.L.F. Holzbaur. 1996. Centractin (ARP1) associates with spectrin revealing a potential mechanism to link dynactin to intracellular organelles. *J. Cell Biol.* 135:1815–1829.

Keller, T.C.S., III, K.A. Conzelman, R. Chasan, and M.S. Mooseker. 1985. Role of myosin in terminal web contraction in isolated epithelial brush borders. *J. Cell Biol.* 100:1647–1655.

Kiehart, D.P., and R. Feghali. 1986. Cytoplasmic myosin from *Drosophila melanogaster*. *J. Cell Biol.* 103:1517–1525.

Knust, E., and M. Leptin. 1996. Adherens junctions in the *Drosophila* embryo: the role of E-cadherin in their establishment and morphogenetic function. *Bioessays*. 18:609–612.

Lazarides, E., W.J. Nelson, and T. Kasamatsu. 1984. Segregation of two spectrin forms in the chicken optic system: a mechanism for establishing restricted membrane-cytoskeletal domains. *Cell*. 36:269–278.

Lee, J.K., E. Brandin, D. Branton, and L.S.B. Goldstein. 1997. α-Spectrin is required for ovarian follicle monolayer integrity in *Drosophila melanogaster*. *Development (Camb.)*. 124:353–362.

Lee, J.K., R.S. Coyne, R.R. Dubreuil, L.S.B. Goldstein, and D. Branton. 1993. Cell shape and interaction defects in α-spectrin mutants of *Drosophila melanogaster*. *J. Cell Biol.* 123:1797–1809.

Lindsley, D.L., and G.G. Zimm. 1992. The Genome of *Drosophila melanogaster*. Academic Press, Inc., San Diego, CA. 1133 pp.

Lombardo, C.R., D.L. Rimm, E. Koslov, and J.S. Morrow. 1994. Human recombinant α-catenin binds to spectrin. *Mol. Biol. Cell*. 5s:47a.

Mahowald, A.P. 1972. Ultrastructural observations on oogenesis in *Drosophila*. *J. Morphol.* 137:29–48.

Matsuoka, Y., C.A. Hughes, and V. Bennett. 1996. Adducin regulation. *J. Biol. Chem*. 271:25157–25166.

McKeown, C., V. Praitis, and J. Austin. 1998. *sma-1* encodes a β_H-spectrin homolog required for *Caenorhabditis elegans* morphogenesis. *Development (Camb.)*. 125:2087–2098.

McNeill, H., M. Ozawa, R. Kemler, and W.J. Nelson. 1990. Novel function of the cell adhesion molecule uvomorulin as an inducer of cell surface polarity. *Cell*. 62:309–316.

Montell, D.J., P. Rorth, and A.C. Spradling. 1992. *slow border cells*, a locus re-

quired for a developmentally regulated cell migration during oogenesis, encodes *Drosophila* C/EBP. *Cell*. 71:51–62.

Morgan, N.S., M.B. Heintzelman, and M.S. Mooseker. 1995. Characterization of myosin-IA and myosin-IB, two unconventional myosins associated with the *Drosophila* brush border cytoskeleton. *Dev. Biol.* 172:51–71.

Nelson, W.J., E.M. Shore, A.Z. Wang, and R.W. Hammerton. 1990. Identification of a membrane-cytoskeletal complex containing the cell adhesion molecule uvomorulin (E-cadherin), ankyrin, and fodrin in Madin-Darby canine kidney epithelial cells. *J. Cell Biol.* 110:349–357.

Niewiadomska, P., D. Godt, and U. Tepass. 1999. *D*E-cadherin is required for intercellular motility during *Drosophila* oogenesis. *J. Cell Biol.* 144:533–547.

Oda, H., T. Uemura, and M. Takeichi. 1997. Phenotypic analysis of null mutants for DE-cadherin and armadillo in *Drosophila* ovaries reveals distinct aspects of their functions in cell adhesion and cytoskeletal organization. *Genes Cells*. 2:29–40.

Patel, N., P.M. Snow, and C.S. Goodman. 1987. Characterization and cloning of fasciclin III: a glycoprotein expressed on a subset of neurons an axon pathways in *Drosophila*. *Cell*. 48:975–988.

Sadler, T.W., K. Burridge, and J. Yonker. 1986. A potential role for spectrin during neurulation. *J Embryol. Exp. Morphol.* 94:73–82.

Sikorski, A.F., G. Terlecki, I.S. Zagon, and S.R. Goodman. 1991. Synapsin I–mediated interaction of brain spectrin with synaptic vesicles. *J. Cell Biol.* 114:313–318.

Speicher, D.W., and V.T. Marchesi. 1984. Erythrocyte spectrin is comprised of many homologous triple helical segments. *Nature*. 311:177–180.

Spradling, A.C. 1993. Developmental genetics of oogenesis. *In* The Development of *Drosophila melanogaster*. Vol. 1. M. Bate and A. Martinez-Arias, editors. Cold Spring Harbor Laboratory Press, Plainview, NY. 1–70.

Spradling, A.C., M. de Cuevas, D. Drummond-Barbosa, L. Keyes, M. Lilly, M. Pepling, and T. Xie. 1997. The *Drosophila* germarium: stem cells, germ line cysts, and oocytes. *Cold Spring Harbor Symp. Quant. Biol.* LXII:25–34.

Thomas, G.H., and D.P. Kiehart. 1994. β_{Heavy}-spectrin has a restricted tissue and sub cellular distribution during *Drosophila* embryogenesis. *Development (Camb.)*. 120:2039–2050.

Thomas, G.H., E.C. Newbern, C.C. Korte, M.A. Bales, S.V. Muse, A.G. Clark, and D.P. Kiehart. 1997. Intragenic duplication and divergence in the spectrin superfamily of proteins. *Mol. Biol. Evol.* 14:1285–1295.

Thomas, G.H., and J.A. Williams. 1999. Dynamic rearrangement of the spectrin membrane skeleton during the generation of epithelial polarity in *Drosophila*. *J. Cell Sci.* 112:2843–2852.

Thomas, G.H., D.C. Zarnescu, A.E. Juedes, M.A. Bales, A. Londergan, C.C. Korte, and D.P. Kiehart. 1998. β_H-spectrin is essential for development and contributes to specific cell fates in the eye. *Development. (Camb.)*. 125:2125–2134.

Uemura, T., H. Oda, R. Kraut, S. Hayashi, Y. Kotaoka, and M. Takeichi. 1996. Zygotic *Drosophila* E-cadherin expression is required for processes of dynamic epithelial cell rearrangement in the *Drosophila* embryo. *Genes Dev.* 10:659–671.

Viel, A., and D. Branton. 1996. Spectrin: on the path from structure to function. *Curr. Opin. Cell Biol.* 8:49–55.

Walker, G.R., R. Kane, and D.R. Burgess. 1994. Isolation and characterization of a sea urchin zygote cortex that supports in vitro contraction and reactivation of furrowing. *J. Cell Sci.* 107:2239–2248.

Wessel, G.M., and S.W. Chen. 1993. Transient, localized accumulation of alpha-spectrin during sea urchin morphogenesis. *Dev. Biol.* 155:161–171.

Wharton, K.A., K.M. Johansen, T. Xu, and S. Artavanis-Tsakonas. 1985. Nucleotide sequence from the neurogenesis locus Notch implies a gene product that shares homology with proteins containing EGF-like repeats. *Cell*. 43: 567–581.

Xu, T., L.A. Caron, R.G. Fehon, and S. Artavanis-Tsakonas. 1992. The involvement of the Notch locus in *Drosophila* oogenesis. *Development (Camb.)*. 115:913–922.

Xu, Y., and G.M. Rubin. 1993. Analysis of genetic mosaics in developing and adult *Drosophila* tissues. *Development (Camb.)*. 117:1223–1237.

Yan, Y., E. Winograd, A. Viel, T. Cronin, S.C. Harrison, and D. Branton. 1993. Crystal structure of the repetitive segments of spectrin. *Science*. 262:2027–2030.

Yeaman, C., K. Grindstaff, and W.J. Nelson. 1999. New perspectives on mechanisms involved in generating epithelial cell polarity. *Physiol. Rev.* 79:73–98.